How to cite: *Angew. Chem. Int. Ed.* **2025**, *64*, e202422882
doi.org/10.1002/anie.202422882

VIP **Electrocatalysis** **Very Important Paper**

Hybrid Enzyme-Electrocatalyst Cascade Modified Gas-Diffusion Electrodes for Methanol Formation from Carbon Dioxide

Panpan Wang[+], Xin Wang[+], Shubhadeep Chandra, Anna Lielpetere, Thomas Quast, Felipe Conzuelo, and Wolfgang Schuhmann**

Abstract: We propose a hybrid electrocatalytic-bioelectrocatalytic reaction cascade integrated on a gas diffusion electrode for CO_2 reduction under selective formation of methanol. Ag-Bi_2O_3 selectively reduces gaseous CO_2 to formate at neutral pH conditions. A subsequent enzymatic cascade comprising formaldehyde dehydrogenase and alcohol dehydrogenase, which are both nicotinamide adenine dinucleotide (NAD)-dependent, further reduce formate sequentially to formaldehyde and methanol. The enzymatically oxidized redox cofactor NAD^+ is regenerated through the enzyme diaphorase which is electrochemically coupled to the electrode by embedding it into a cobaltocene-based low-potential redox polymer. Methanol formation is confirmed using a highly selective biosensor based on alcohol oxidase in combination with horseradish peroxidase integrated into a specifically adapted redox polymer. The proposed hybrid electrocatalytic-bioelectrocatalytic cascade is an example for a general strategy for enhancing the selectivity of electrocatalytic reactions and/or to replace bioelectrochemically challenging steps such as the synthesis of formate from CO_2 using highly oxygen-sensitive formate dehydrogenases by more robust inorganic electrocatalysts.

Introduction

The development of technologies for the conversion of excess atmospheric CO_2 undoubtedly constitutes an important field of research. In this regard, the possibility to use CO_2 as a feedstock for the synthesis of fuels or value-added products results in a double reward, not only sequestrating CO_2 but also contributing to the creation of circular and sustainable economic strategies. Consequently, great efforts have been directed to the development of catalysts enabling CO_2 conversion,[1] including heterogeneous catalysis,[2] photocatalysis,[3] and electrocatalysis,[4] among others. In particular, enzymatic conversion systems[5] have advantages concerning attractive conditions, as they operate in aqueous solutions, at ambient temperature and near neutral pH.

Enzymatic conversion of CO_2 to methanol was described by cooperative action of the enzymes formate dehydrogenase (FDH) and methanol dehydrogenase in an electrochemical approach, using either pyrroloquinoline quinone or methyl viologen as electron mediators.[6] A subsequent report showed a more efficient conversion by coupling three different nicotinamide adenine dinucleotide (NADH)-dependent dehydrogenases for the sequential $6\,e^-$ reduction process:[7] CO_2 to formate catalyzed by FDH, formate to formaldehyde catalyzed by formaldehyde dehydrogenase (FaDH), and formaldehyde to methanol catalyzed by alcohol dehydrogenase (ADH). Since then, the cascade reaction involving the three dehydrogenase enzymes has been widely investigated, using different approaches for integrating biomolecules, adapting reaction conditions, and improving cofactor regeneration.[8] Although highly appealing, in this enzymatic cascade each conversion process proceeds against the thermodynamic preferred direction of the naturally catalyzed enzymatic reactions.[9]

The last enzyme in the conversion cascade, ADH, is known for its low affinity towards methanol (K_M = 130 mM[10]). The reverse reaction is more efficient with a comparatively higher affinity for formaldehyde (K_M = 6 mM[8]). As a result, formaldehyde reduction is almost irreversible, and the equilibrium of the reaction is naturally shifted to methanol production. In contrast, formate reduction catalyzed by FaDH is the limiting step of the cascade because the equilibrium is on the formate side, hence requiring an accumulation of relatively high formate concen-

[*] Dr. P. Wang,[+] Dr. X. Wang,[+] Dr. S. Chandra, Dr. A. Lielpetere, Dr. T. Quast, Prof. Dr. W. Schuhmann
Analytical Chemistry – Center for Electrochemical Sciences (CES), Faculty of Chemistry and Biochemistry, Ruhr University Bochum
Universitätsstr. 150, D-44780 Bochum, Germany
E-mail: wolfgang.schuhmann@rub.de

Dr. F. Conzuelo
Instituto de Tecnologia Química e Biológica António Xavier, Universidade Nova de Lisboa
Av. da República, 2780-157 Oeiras, Portugal
E-mail: felipe.conzuelo@itqb.unl.pt

Dr. A. Lielpetere
Present address: Latvian Institute of Organic Synthesis
Aizkraukles Street 21, LV-1006 Riga, Latvia

[+] These authors contributed equally to this work.

trations ensuring FaDH catalysis in the reduction direction.[8,11] Moreover, a relatively high initial concentration of NADH is needed to increase the biocatalytic reduction.[9] However, excess NADH has been found to have an inhibitory effect especially for the initial step of CO_2 reduction to formate by means of FDH.[8]

With the aim to overcome these limitations, we investigated the possibility of replacing the enzyme FDH in the cascade with an inorganic catalyst capable of performing the selective and efficient reduction of CO_2 to formate (Scheme 1). This strategy would prevent the inhibition of FDH by NADH required in the enzymatic cascade and would ensure the high local formate concentrations required for methanol production. We present a hybrid electrocatalytic/bioelectrocatalytic system combining an inorganic catalyst with a bienzymatic cascade for CO_2 electroreduction. The inorganic catalyst is supported on a gas diffusion layer and enables the selective conversion of CO_2 to formate with high conversion yields. The generated formate is then sequentially converted in a two-step process catalyzed by the two NADH-dependent enzymes, FaDH and ADH, via formaldehyde to methanol. NADH regeneration is ensured by an additional enzyme, diaphorase (DIA), which is wired to the electrode surface in a mediated electron transfer regime by means of a redox polymer, allowing NAD^+ reduction at the same applied potential as required for the electrocatalytic CO_2 reduction.

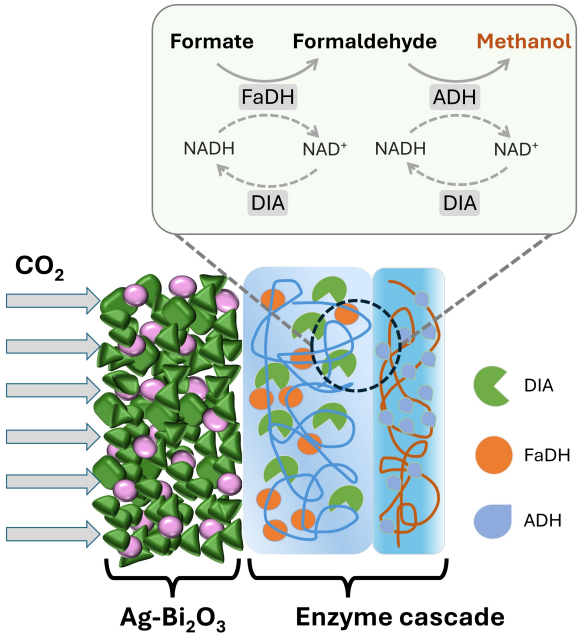

Scheme 1. Hybrid electrocatalytic-bioelectrocatalytic cascade integrated on a gas diffusion electrode for CO_2 reduction under selective formation of methanol. CO_2 is first converted to formate in an electrocatalytic step catalyzed by Ag-Bi_2O_3. Subsequently, formate is converted in a bioelectrocatalytic reaction by the enzymes formaldehyde dehydrogenase (FaDH) and alcohol dehydrogenase (ADH) to obtain methanol as the final product. Regeneration of the cofactor NADH is achieved electrochemically through diaphorase (DIA) embedded and electronically wired in a redox polymer.

Results and Discussion

Electrochemical CO_2 Reduction

An inorganic catalyst consisting of Ag-Bi_2O_3 hybrid nanofibers on a gas-diffusion electrode (GDE) exhibiting efficient electrochemical reduction of CO_2 to formate, as shown previously,[12] was selected as the first catalyst for the overall CO_2 reduction cascade. The Ag-Bi_2O_3 catalyst was immobilized on hydrophobic carbon paper acting as a gas-diffusion layer for alleviating the CO_2 mass transport limitation caused by the low CO_2 solubility in aqueous solutions, thus increasing the CO_2 conversion rate. This catalyst was initially developed and characterized for operation in alkaline solutions (1.0 M KOH).[12] However, with the aim of integrating this catalyst with an enzymatic conversion system as shown in Scheme 1, the material was now investigated under conditions that are compatible with the enzyme-catalyzed conversion. The electrochemical performance of Ag-Bi_2O_3-modified GDEs was evaluated in 0.1 M phosphate buffer at pH 7.0. A flow-through cell with a small electrolyte volume (5 mL) facilitated achieving increased concentrations of the formed products. Chronopotentiometric measurements were performed by applying different current densities, and the products were quantified by means of HPLC. Figure 1 shows the Faradaic efficiencies (FE) of the reduction of CO_2 at the Ag-Bi_2O_3-modified GDE at neutral conditions in a current density range from -25 to -400 mA cm^{-2}. The high selectivity of (95 ± 3)% for the FE of formate formation could be confirmed with low FE for CO of below 3 % in the whole investigated range, and a competitive hydrogen evolution reaction of below 1 % for current densities exceeding 25 mA cm^{-2}. These results confirmed the suitability of the inorganic catalyst Ag-Bi_2O_3

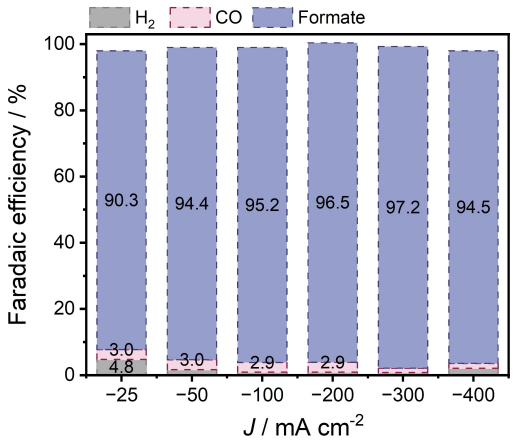

Figure 1. Faradaic efficiency for the CO_2 reduction reaction performed with a GDE constituted of Ag-Bi_2O_3 nanofibers on a hydrophobic carbon paper. Each current density was applied for 870 s. Gas and liquid products were analyzed by gas chromatography (GC) and high-performance liquid chromatography (HPLC), respectively. Electrolyte: 0.1 M phosphate buffer, pH 7.0. A CO_2 gas stream was supplied to the backside of the GDE at a flow rate of 20 mL min^{-1}. A N_2 gas stream was used to saturate the electrolyte in the cathode compartment at a flow rate of 20 mL min^{-1}.

for the close-to-quantitative conversion of CO_2 into formate as the initial step of the envisaged hybrid cascade, even at neutral pH conditions.

Bioelectrocatalytic NADH Regeneration

Both dehydrogenases (FaDH and ADH) used in the enzymatic cascade are NADH-dependent enzymes. Hence, it was necessary to implement an efficient NADH regeneration system to ensure the sequential conversion of intermediates leading to the final desired product, i.e., methanol. Electrochemical NAD^+ reduction is highly appealing for this purpose, as the use of a reducing agent is replaced by an electrochemically-driven reaction and water serves as the proton source.[13] It is important to obtain the biologically active form of NADH during regeneration (1,4-NADH) which is indispensably required for the enzyme-catalyzed reactions instead of biologically inactive isomers and dimers which are usually produced in large amounts by direct reaction at the electrode surface at very negative potentials.[14] Diaphorases (DIA) are enzymes catalyzing the interconversion between NAD^+ and NADH, and it has been shown that NADH regeneration in a mediated electron transfer regime is possible when a suitable DIA is immobilized and wired using redox polymer matrices.[15,16] Considering the standard redox potential of the NAD^+/NADH redox couple (−0.32 V vs. SHE),[16] two low-potential redox polymers were synthesized and investigated for the immobilization and electrical wiring of DIA. The redox polymers included the viologen-modified polymer poly(3-azido-propyl methacrylate-*co*-glycidyl methacrylate)-1-(hex-5-yn-1-yl)-1'-methyl-[4,4'-bipyridinium] (*co*P(N_3MA-GMA)-vio, Figure S2a) and a cobaltocene derivative bound to branched polyethylenimine (BPEI-[$CoCp_2$], Figure S2b). DIA was integrated into each of the two redox polymer matrices and deposited on glassy carbon electrodes. The modified electrodes were characterized by cyclic voltammetry in Ar-saturated conditions in the absence and presence of 10 mM NAD^+. Moreover, amperometric measurements were also recorded before and after NAD^+ addition (Figure 2). The midpoint potentials of the investigated redox polymers were −0.280 V vs. SHE for the viologen-modified polymer *co*P(N_3MA-GMA)-vio (Figure 2a) and −0.600 V vs. SHE for BPEI-[$CoCp_2$] (Figure 2c). The voltammetric responses and amperograms upon addition of NAD^+ clearly confirmed that mediated electron transfer between the redox polymer and the integrated DIA is possible allowing electroenzymatic NAD^+ reduction. The catalytic reduction reaction rate was directly related to the potential difference between the redox polymer midpoint potential and the NAD^+/NADH redox couple. As a result, BPEI-[$CoCp_2$] was chosen as the most suitable redox polymer, providing sufficient driving force for the electron transfer to DIA and hence leading to 25 times higher catalytic currents for NAD^+ reduction.

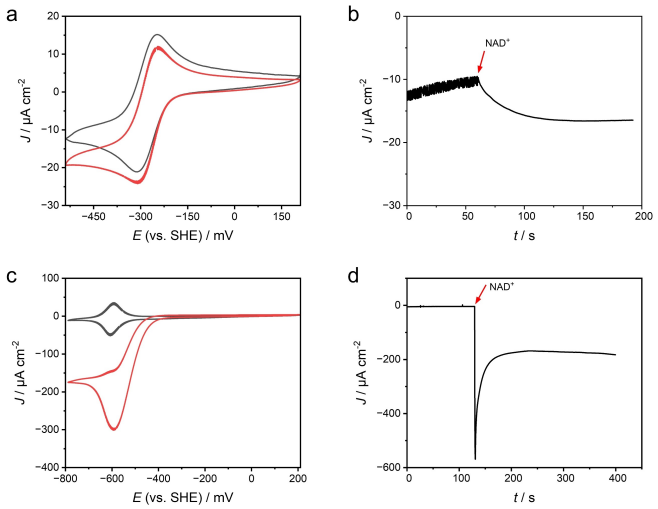

Figure 2. Electrochemical characterization of DIA embedded into low-potential redox polymers. a, b) Viologen-modified redox polymer (*co*P(N_3MA-GMA)-vio). c, d) Cobaltocene-modified redox polymer (BPEI-[$CoCp_2$]). Ar-saturated 0.1 M phosphate buffer, pH 7.0. a, c) Cyclic voltammograms recorded in the absence (black trace) and presence (red trace) of 10 mM NAD^+. Scan rate: 2 mV s^{-1}. b, d) Amperometric responses at an applied potential of −540 mV vs. SHE (panel b), and −590 mV vs. SHE (panel d). The red arrow indicates the addition of 10 mM NAD^+.

NADH Regeneration by Combining Redox-Polymer-Integrated Diaphorase and Alcohol Dehydrogenase

The NADH regeneration system was evaluated in combination with NADH-dependent alcohol dehydrogenase for the conversion of formaldehyde to methanol. A glassy-carbon electrode modified with DIA embedded within the cobaltocene-modified redox polymer was coated with an additional layer consisting of ADH integrated within the redox-silent zwitterionic polymer poly(2-methacryloyloxyethyl phosphorylcholine-*co*-glycidyl methacrylate (MPC, Figure S3). This polymer was previously used as a stable immobilization matrix for the entrapment of redox-active enzymes and at the same time allowing the diffusion of small molecules into the polymer matrix.[17] To confirm the operation of the bioelectrode for efficient NADH regeneration in the presence of the additional layer, cyclic voltammograms for the ADH/MPC/DIA/BPEI-[$CoCp_2$]-modified electrode were performed in the absence and presence of NAD^+ (Figure 3a).

The catalytic current in the presence of NAD^+ indicated a similar performance as that observed for the DIA/BPEI-[$CoCp_2$]-modified electrodes, confirming successful NADH regeneration. In agreement with previous reports for reductive enzyme cascades using these enzymes,[8,10] the optimum pH for the cascade conversion was pH 7 (Figure S4). Aiming at the reduction of aldehydes to their corresponding alcohols by ADH, in particular to the formation of methanol, the catalytic current was monitored at a constant applied potential of −690 mV vs. SHE in the presence of NADH after the addition of formaldehyde. As shown in Figure 3b (red trace), an increase in the cathodic current was observed

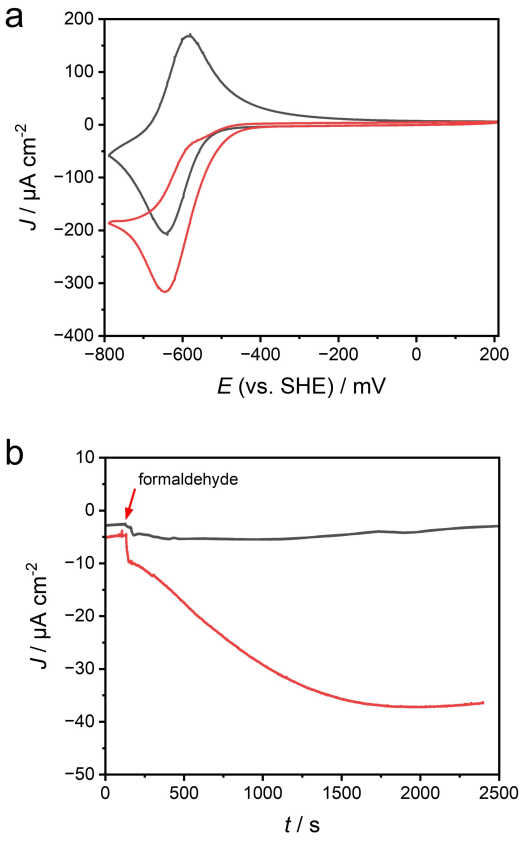

Figure 3. Characterization of ADH/MPC/DIA/BPEI-[$CoCp_2$]-modified electrodes. a) Cyclic voltammograms in the absence (black trace) and presence (red trace) of 10 mM NAD^+. Scan rate: 5 mV s^{-1}. b) Amperometric responses at an applied potential of −690 mV vs. SHE, in the absence (black trace) and presence (red trace) of 2 mM NADH. The red arrow indicates the addition of 10 mM formaldehyde. For both panels, electrolyte: Ar-saturated 0.1 M phosphate buffer, pH 7.0.

upon formaldehyde addition due to the reduction of formaldehyde to methanol by ADH under simultaneous oxidation of NADH to NAD^+, which is in turn regenerated by means of the cobaltocene-modified redox-polymer-wired DIA. A control experiment performed in the absence of NADH (see Figure 3b, black trace) showed a negligible increase in cathodic current, which was below 1 % with respect to the previous response, and possibly ascribed to traces of O_2 introduced into the electrochemical cell during substrate addition. As the NADH cofactor was absent in this case, the reduction of formaldehyde by ADH was not possible, and no sustained catalytic current was observed, confirming the functioning of the NADH regeneration system for the reduction of formaldehyde to methanol. An important factor to consider in the development of the hybrid cascade system for methanol formation from CO_2 is the possible impact of formaldehyde on the activity of the used enzymes. The accumulation of the highly reactive intermediate formaldehyde could affect the conversion efficiency by disrupting the protein structures of the biocatalysts.[18] Hence, the catalytic current for NAD^+ reduction by redox-polymer-wired DIA was investigated after the addition of formaldehyde in a relatively large concentration. The activity of DIA was significantly affected by the presence of formaldehyde (see Figure S5), causing a gradual decrease of the catalytic current for NAD^+ reduction over consecutive voltammetric cycles. The recorded currents decreased to 40 % of the initial response after the first cycle in the presence of formaldehyde and below 20 % for consecutive cycles. Thus, it was important to ensure a high relative activity of ADH with respect to the rate for formaldehyde production by FaDH to prevent the accumulation of the harmful intermediate.

Integration of Formaldehyde Dehydrogenase into the Hybrid Cascade

The NADH-dependent enzyme FaDH was co-immobilized with DIA into the BPEI-[$CoCp_2$] redox polymer and applied for the conversion of formate to formaldehyde. As before, the modified electrode was characterized by amperometry at an applied potential that ensures NADH regeneration. An increase in cathodic current was observed after the addition of formate to the electrochemical cell (Figure S6), confirming the reduction reaction catalyzed by FaDH, with the resulting NAD^+ being reduced by DIA, which is electrically wired by the BPEI-[$CoCp_2$] redox polymer to the electrode. The relatively low catalytic current observed after the addition of formate (about 7 % with respect to formaldehyde reduction by ADH) was attributed to the limited activity of FaDH, which is about 90 times lower than that of ADH. In consequence, the efficiency of the overall cascade reaction for CO_2 conversion to methanol is limited by the intermediate step from formate to formaldehyde. However, this simultaneously assures that formaldehyde accumulation is prevented, which, as shown before, has a negative impact on DIA activity.

Hybrid Cascade for Methanol Production

The compatibility between the inorganic catalyst and the enzymatic conversion system was assessed by the combination of the Ag-Bi_2O_3 GDE with the NADH regeneration system. A piece of porous hydrophilic carbon cloth was used for the immobilization of DIA/BPEI-[$CoCp_2$], which was placed on top of the Ag-Bi_2O_3 catalyst gas-diffusion layer. In this way, an electrical connection was established between both carbon layers, constituting an integrated hybrid electrode. Moreover, the diffusion of formate generated during electrochemical CO_2 reduction to reach the enzymatic layer was ensured. The assembly was characterized by cyclic voltammetry in the presence of CO_2 flowing to the back side of the hybrid GDE. The electrochemical response confirmed the reduction of CO_2 while also revealing the characteristic redox response of the cobaltocene-modified redox polymer, centered at −600 mV vs. SHE (Figure S7). Even when more negative potentials were applied to the electrode, the integration of DIA in the cobaltocene-modified redox polymer ensured mediated electron transfer between DIA and the carbon layer. The electrolyte solution was analyzed

by high-performance liquid chromatography (HPLC) before and after the voltammetric characterization showing the formation of formate as a result of electrochemical CO_2 reduction (Figure 4), in agreement with the retention time observed in the analysis of formate standards (Figure S8). These results also confirmed the activity of the Ag-Bi_2O_3 catalyst for CO_2 reduction after adding the biocatalytic layer.

The complete hybrid cascade was established by additional integration of the enzymes FaDH and ADH. FaDH and DIA were embedded into the BPEI-[$CoCp_2$] redox polymer layer, while ADH was embedded in the zwitterionic polymer (MPC) and deposited on top of the BPEI-[$CoCp_2$] redox polymer layer. Formate generated by the inorganic Ag-Bi_2O_3 catalyst is reduced by FaDH to formaldehyde, which is further reduced to methanol by ADH. Simultaneously, both dehydrogenases produce NAD^+, which is reduced by the BPEI-[$CoCp_2$] redox polymer-wired DIA to regenerate the NADH cofactor. To further investigate the performance of the overall cascade, the reduction reaction was monitored at different applied potentials (Figure 5). At an applied potential of −890 mV vs. SHE, the electrode showed a rather stable current output throughout 2 h. Subsequently, the electrode was polarized at −990 mV and

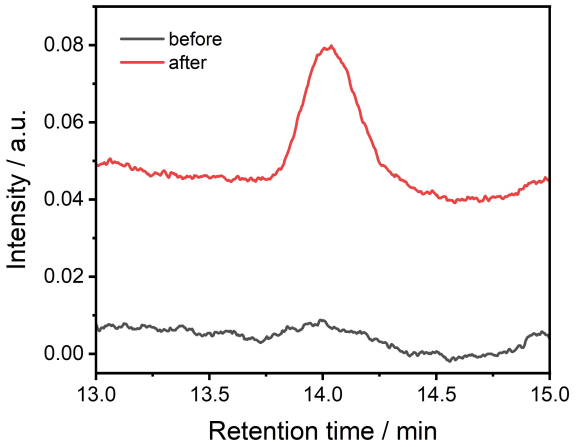

Figure 4. a) Chromatograms obtained from the HPLC analysis of the electrochemical conversion products for a DIA/BPEI-[$CoCp_2$]/Ag-Bi_2O_3/GDE. Results obtained for samples taken before and after cyclic voltammetry, as shown in Figure S7.

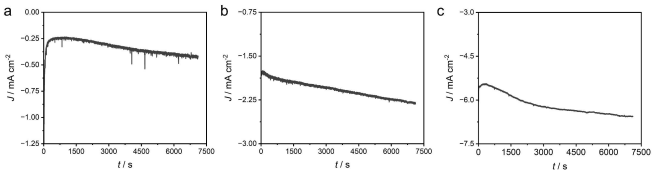

Figure 5. Chronoamperometric responses for an ADH/MPC/FaDH/DIA/BPEI-[$CoCp_2$]/Ag-Bi_2O_3/GDE at different applied potentials vs. SHE: −890 mV (a), −990 mV (b), −1090 mV (c). Electrolyte: 0.1 M phosphate buffer, pH 7.0, containing 10 mM NADH. A CO_2 gas stream was supplied to the backside of the GDE at a flow rate of 20 mL min^{-1}. A N_2 gas stream was used to saturate the electrolyte in the cathode compartment at a flow rate of 20 mL min^{-1}.

−1090 mV (vs. SHE), providing increasing catalytic currents. No formate production was observed with the Ag-Bi_2O_3-modified GDE at potentials more positive than −890 mV vs. SHE. Thus, this potential was selected as optimum for the operation of the hybrid electrocatalytic/bioelectrocatalytic cascade.

The electrolyte solution was analyzed after the electrochemical conversion using an enzyme-based alcohol biosensor for the selective quantification of methanol. The biosensor was fabricated by co-immobilizing the enzymes horseradish peroxidase (HRP) and alcohol oxidase (AOX) within an Os-complex-modified redox polymer matrix (P–Os, Figure S9a).[19] With the biosensor, methanol is oxidized by AOX in the presence of O_2 to produce H_2O_2, which is then reduced by HRP under mediated electron transfer with the electrode surface via the P–Os redox polymer (Figure S9b).[20]

Figure S10 shows a comparison of voltammetric responses for the biosensor in the absence and presence of methanol. The expected cathodic response for H_2O_2 reduction was observed in the presence of methanol. The biosensor was also characterized at a constant applied potential after the addition of varying methanol concentrations to the electrolyte solution, showing the possibility of detecting methanol in concentrations as low as 5 μM (Figure S11).

A sample collected after CO_2 conversion with the hybrid GDE was analyzed with the biosensor. After the addition of the sample aliquot, an increase in cathodic current was observed, indicating methanol conversion (Figure 6a). This result confirmed the formation of the envisaged product methanol as the terminal product of the hybrid cascade. As a control experiment, the electrolyte solution was also analyzed before CO_2 conversion. In the latter case, an anodic current response was observed (Figure 6b), which could be explained by the oxidation of NADH at the biosensor surface due to the comparatively high applied potential. The possible co-oxidation of NADH prevented the exact quantification of methanol; however, the detected cathodic current unequivocally confirms the generation of methanol with the hybrid cascade for the conversion of CO_2.

Conclusions

We have demonstrated the exemplary implementation of a hybrid electrocatalytic/bioelectrocatalytic reaction cascade for the selective multi-step reduction of carbon dioxide to methanol. The system integrates a gas-diffusion electrode modified with an inorganic catalyst, Ag-Bi_2O_3, for the efficient and selective electrochemical reduction of CO_2 to formate with about 95 % Faradaic efficiency in neutral pH, ensuring compatibility with the coupled enzymatic reactions as well as the integrity of the enzymes. An enzymatic cascade was used for the sequential conversion of formate to formaldehyde and finally to methanol by consecutive action of two NADH-dependent enzymes, i.e., FaDH and ADH. NADH regeneration was achieved by a third enzyme (DIA) wired to the electrode in a mediated electron transfer regime

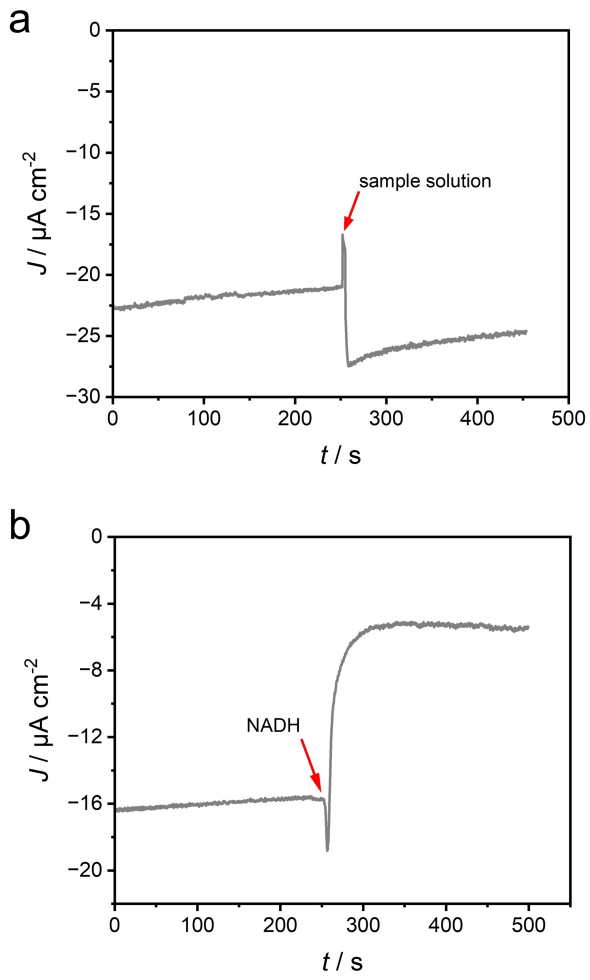

Figure 6. Methanol detection after CO_2 conversion with the complete hybrid reaction cascade using an AOX/HRP-based biosensor. a) Analysis of an aliquot of the electrolyte solution collected after CO_2 electrolysis with the complete hybrid cascade. b) Control experiment showing the biosensor response upon addition of 5 mM NADH. Amperometric measurements with a glassy carbon electrode modified with AOX and HRP embedded in P–Os at an applied potential of 210 mV vs. SHE. Electrolyte: 0.1 M phosphate buffer, pH 7.0. The red arrow indicates the time for sample addition.

using a cobaltocene-based low-potential redox polymer. The limiting step in the process is the one catalyzed by the enzyme FaDH, due to its substantially lower activity in comparison with the other catalytic conversions, suggesting that the performance of the cascade reaction could be improved by replacing FaDH with a variant showing higher activity. Nevertheless, the fact that this is the limiting step of the reaction is advantageous as the accumulation of formaldehyde is prevented avoiding enzyme activity loss. This constitutes the first example of a hybrid electrocatalytic/bioelectrocatalytic reaction cascade using a gas-diffusion electrode. The hybrid cascade strategy has advantages of overcoming previously observed constraints when using formate dehydrogenase for the initial enzymatic conversion of CO_2, which is highly oxygen sensitive and yields comparatively small amounts of formate, thus limiting the overall cascade. With the hybrid cascade, large amounts of formate are produced, driving the enzymatic reactions in the desired reduction direction for methanol production. The cascade presents the advantage of integrating all catalysts in a heterogeneous system, ensuring a straightforward separation from the reaction media. However, downstream product separation is still required due to the presence of the redox cofactor in solution. In views of potential future applications, the system ought to be optimized to maximize methanol production and ideally replace the biocatalytsts by NADH-independent dehydrogenases.

Acknowledgements

Financial support by the European Research Council (ERC) under the European Union's Horizon 2020 research and innovation programme (CasCat [833408]) and FCT – Fundação para a Ciência e a Tecnologia, I.P. through grant [2022.07024.PTDC] is acknowledged. F.C. is grateful to FCT for the researcher contract [2022.05842.CEECIND/CP1725/CT0001] under the Scientific Employment Stimulus–Individual Call 2022. Open Access funding enabled and organized by Projekt DEAL.

Conflict of Interest

The authors declare no conflict of interest.

Data Availability Statement

The data that support the findings of this study are available from the corresponding author upon reasonable request.

Keywords: CO_2 reduction · electrocatalysis · bioelectrocatalysis · gas-diffusion electrode · redox polymer

[1] S. Sarp, S. Gonzalez Hernandez, C. Chen, S. W. Sheehan, *Joule* **2021**, *5*, 59–76.
[2] a) R.-P. Ye, J. Ding, W. Gong, M. D. Argyle, Q. Zhong, Y. Wang, C. K. Russell, Z. Xu, A. G. Russell, Q. Li, M. Fan, Y.-G. Yao, *Nat. Commun.* **2019**, *10*, 5698; b) X. Jiang, X. Nie, X. Guo, C. Song, J. G. Chen, *Chem. Rev.* **2020**, *120*, 7984–8034; c) L. H. Vieira, L. F. Rasteiro, C. S. Santana, G. L. Catuzo, A. H. M. Da Silva, J. M. Assaf, E. M. Assaf, *ChemCatChem* **2023**, *15*.
[3] a) S. N. Habisreutinger, L. Schmidt-Mende, J. K. Stolarczyk, *Angew. Chem. Int. Ed.* **2013**, *52*, 7372–7408; b) Y. Li, Y. Lei, D. Li, A. Liu, Z. Zheng, H. Liu, J. Guo, S. Liu, C. Hao, D. He, *ACS Catal.* **2023**, *13*, 10177–10204; c) Z. Shang, X. Feng, G. Chen, R. Qin, Y. Han, *Small* **2023**, *19*.
[4] a) S. A. Al-Tamreh, M. H. Ibrahim, M. H. El-Naas, J. Vaes, D. Pant, A. Benamor, A. Amhamed, *ChemElectroChem* **2021**, *8*, 3207–3220; b) P. Dessì, L. Rovira-Alsina, C. Sánchez, G. K. Dinesh, W. Tong, P. Chatterjee, M. Tedesco, P. Farràs, H. M. V. Hamelers, S. Puig, *Biotechnol. Adv.* **2021**, *46*, 107675; c) S. Jin, Z. Hao, K. Zhang, Z. Yan, J. Chen, *Angew. Chem. Int. Ed.* **2021**, *133*, 20627–20648; d) G. Wang, J. Chen, Y. Ding,

P. Cai, L. Yi, Y. Li, C. Tu, Y. Hou, Z. Wen, L. Dai, *Chem. Soc. Rev.* **2021**, *50*, 4993–5061; e) S. Nitopi, E. Bertheussen, S. B. Scott, X. Liu, A. K. Engstfeld, S. Horch, B. Seger, I. E. L. Stephens, K. Chan, C. Hahn, J. K. Nørskov, T. F. Jaramillo, I. Chorkendorff, *Chem. Rev.* **2019**, *119*, 7610–7672; f) L. Luan, X. Ji, B. Guo, J. Cai, W. Dong, Y. Huang, S. Zhang, *Biotechnol. Adv.* **2023**, *63*, 108098; g) C. P. O'Brien, R. K. Miao, A. Shayesteh Zeraati, G. Lee, E. H. Sargent, D. Sinton, *Chem. Rev.* **2024**, *124*, 3648–3693.

[5] a) J. Shi, Y. Jiang, Z. Jiang, X. Wang, X. Wang, S. Zhang, P. Han, C. Yang, *Chem. Soc. Rev.* **2015**, *44*, 5981–6000; b) S. Bierbaumer, M. Nattermann, L. Schulz, R. Zschoche, T. J. Erb, C. K. Winkler, M. Tinzl, S. M. Glueck, *Chem. Rev.* **2023**, *123*, 5702–5754.

[6] S. Kuwabata, R. Tsuda, H. Yoneyama, *J. Am. Chem. Soc.* **1994**, *116*, 5437–5443.

[7] R. Obert, B. C. Dave, *J. Am. Chem. Soc.* **1999**, *121*, 12192–12193.

[8] C. Di Spiridione, M. Aresta, A. Dibenedetto, *Molecules* **2022**, *27*, 4913.

[9] F. Marpani, M. Pinelo, A. S. Meyer, *Biochem. Eng. J.* **2017**, *127*, 217–228.

[10] R. Cazelles, J. Drone, F. Fajula, O. Ersen, S. Moldovan, A. Galarneau, *New J. Chem.* **2013**, *37*, 3721–3730.

[11] J. Luo, A. S. Meyer, R. V. Mateiu, M. Pinelo, *Nat. Biotechnol.* **2015**, *32*, 319–327.

[12] X. Wang, W. He, J. Shi, J. R. C. Junqueira, J. Zhang, S. Dieckhöfer, S. Seisel, D. Das, W. Schuhmann, *Chem. Asian J.* **2023**, *18*, e202201165.

[13] a) S. Immanuel, R. Sivasubramanian, R. Gul, M. A. Dar, *Chem. Asian J.* **2020**, *15*, 4256–4270; b) Y. S. Lee, R. Gerulskis, S. D. Minteer, *Curr. Opin. Biotechnol.* **2021**, *73*, 14–21; c) E. Aamer, J. Thöming, M. Baune, N. Reimer, R. Dringen, M. Romero, I. Bösing, *Sci. Rep.* **2022**, *12*, 16380.

[14] X. Wang, T. Saba, H. H. Yiu, R. F. Howe, J. A. Anderson, J. Shi, *Chem* **2017**, *2*, 621–654.

[15] a) T. Quah, R. D. Milton, S. Abdellaoui, S. D. Minteer, *Chem. Commun.* **2017**, *53*, 8411–8414; b) F. Dong, H. Chen, C. A. Malapit, M. B. Prater, M. Li, M. Yuan, K. Lim, S. D. Minteer, *J. Am. Chem. Soc.* **2020**, *142*, 8374–8382; c) B. Alkotaini, S. Abdellaoui, K. Hasan, M. Grattieri, T. Quah, R. Cai, M. Yuan, S. D. Minteer, *ACS Sustainable Chem. Eng.* **2018**, *6*, 4909–4915.

[16] M. Yuan, M. J. Kummer, R. D. Milton, T. Quah, S. D. Minteer, *ACS Catal.* **2019**, *9*, 5486–5495.

[17] K. Jayakumar, A. Lielpetere, D. A. Domingo-Lopez, R. E. Levey, G. P. Duffy, W. Schuhmann, D. Leech, *Biosens. Bioelectron.* **2023**, *219*, 114815.

[18] a) J. J. A. G. Kamps, R. J. Hopkinson, C. J. Schofield, T. D. W. Claridge, *Commun. Chem.* **2019**, *2*, 126; b) Y. Huang, H. Cai, F. Luo, L. Chen, C. Lin, J. Wang, L. Guo, B. Qiu, Z. Lin, *Biosens. Bioelectron.* **2024**, *267*, 116778.

[19] a) F. Conzuelo, N. Marković, A. Ruff, W. Schuhmann, *Angew. Chem. Int. Ed.* **2018**, *57*, 13681–13685; b) F. Conzuelo, N. Marković, A. Ruff, W. Schuhmann, *Angew. Chem.* **2018**, *130*, 13870–13875.

[20] a) A. Narváez, G. Suárez, I. C. Popescu, I. Katakis, E. Domínguez, *Biosens. Bioelectron.* **2000**, *15*, 43–52; b) A. M. Azevedo, D. M. F. Prazeres, J. M. S. Cabral, L. P. Fonseca, *Biosens. Bioelectron.* **2005**, *21*, 235–247; c) P. Goswami, S. S. R. Chinnadayyala, M. Chakraborty, A. K. Kumar, A. Kakoti, *Appl. Microbiol. Biotechnol.* **2013**, *97*, 4259–4275.

Manuscript received: November 24, 2024
Accepted manuscript online: December 23, 2024
Version of record online: January 3, 2025